

A multi-scale approach for particle-laden viscoelastic flows using a discrete particle method

Célio Fernandes, Salah Aldin Faroughi, Ricardo Ribeiro,
Ana Isabel Roriz, Gareth Huw McKinley

*Institute for Polymers and Composites, University of Minho, Campus de Azurém, 4800-058
Guimarães, Portugal; cbpf@dep.uminho.pt (C.F.); a58714@alunos.uminho.pt (R.R.);
b12374@dep.uminho.pt (A.I.R.)*

*Geo-Intelligence Laboratory, Ingram School of Engineering, Texas State University, San Marcos, Texas,
78666, USA; salah.faroughi@txstate.edu (S.A.F.)*

*Hatsopoulos Microfluids Laboratory, Department of Mechanical Engineering, Massachusetts Institute
of Technology, Cambridge, Massachusetts 02139, USA; gareth@mit.edu (G.H.M.)*

1. Introduction

Accurately resolving the coupled momentum transfer between the liquid and solid phases is a fundamental problem in multiphase transport processes involving complex fluids, such as in hydraulic fracture operations. Specifically, we need to characterize the dependence of the normalized average fluid-particle force $\langle F \rangle$ on the volume fraction ϕ of the dispersed solid phase and on the rheology of the complex fluid matrix, parameterized through the Weissenberg number Wi measuring the relative magnitude of elastic to viscous stresses in the fluid.

2. Governing equations

The basic equations governing transient, incompressible and isothermal laminar flows of viscoelastic fluids are the continuity, momentum and constitutive equations. The continuity and momentum equations read:

$$\nabla \cdot (\rho \mathbf{u}) = 0,$$

$$\partial(\rho \mathbf{u})/\partial t + \nabla \cdot (\rho \mathbf{u} \mathbf{u}) + \nabla \cdot (p \mathbf{I}) - \nabla \cdot \boldsymbol{\tau} = 0,$$

where ρ is the fluid density, \mathbf{u} is the velocity vector, t is the time, p is the pressure, \mathbf{I} is the identity tensor and $\boldsymbol{\tau}$ is the total extra-stress tensor, which is split into solvent $\boldsymbol{\tau}_S$ and polymeric $\boldsymbol{\tau}_P$ contributions, such that $\boldsymbol{\tau} = \boldsymbol{\tau}_S + \boldsymbol{\tau}_P$. Both stress terms are obtained by the following equations, which form the constitutive model,

$$\boldsymbol{\tau}_S = \eta_S(\nabla\mathbf{u} + \nabla\mathbf{u}^T),$$

$$\lambda \overset{\nabla}{\boldsymbol{\tau}}_P + \boldsymbol{\tau}_P = \eta_P (\nabla\mathbf{u} + \nabla\mathbf{u}^T),$$

where η_S and η_P are the solvent and polymeric viscosities, respectively, λ is the fluid relaxation time and $\overset{\nabla}{\boldsymbol{\tau}}_P$ indicates the upper-convective time derivative of the polymeric extra-stress tensor defined as

$$\overset{\nabla}{\boldsymbol{\tau}}_P \equiv \partial\boldsymbol{\tau}_P/\partial t + \mathbf{u} \cdot \nabla\boldsymbol{\tau}_P - \boldsymbol{\tau}_P \cdot \nabla\mathbf{u} - \nabla\mathbf{u}^T \cdot \boldsymbol{\tau}_P.$$

For this model, a characteristic (polymeric) viscosity ratio can be defined by $\zeta = \eta_P/(\eta_S + \eta_P) = \eta_P/\eta_0$, known as retardation ratio, where η_0 is the total viscosity in the limit of vanishing shear rate.

3. Case studies

In order to develop our computational methodology, we address only non-colloidal suspensions with viscoelastic matrices, and focus on both dilute and moderately dense suspensions. Following Housiadas and Tanner [1], we consider the effect of other particles in the flow, by assuming that from the point of view of a single particle at any instant, the remaining particles act like a porous medium. Fig. 1 illustrates schematically the computational domain, which is used here to simulate the steady-state flow of unbounded viscoelastic fluids around random arrays of spheres.

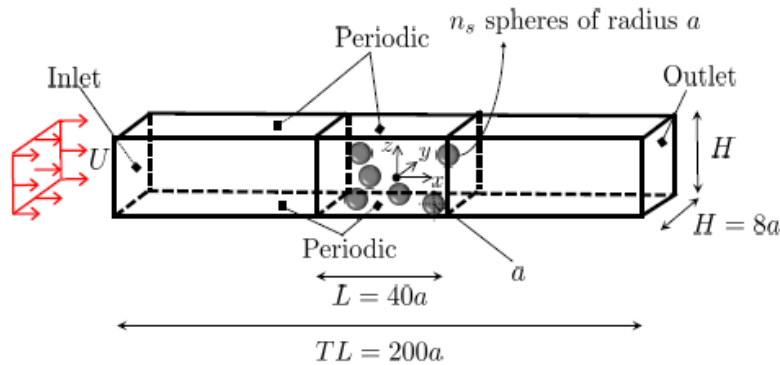


Figure 1. Schematic of the channel cross-section used for DNS of random arrays of spheres immersed in Newtonian and quasi-linear Oldroyd-B viscoelastic fluids. The particle volume fractions considered include $\phi = 0.04, 0.08, 0.12, 0.16$ and 0.20 .

3.1. Verification: Stokes flow of suspensions with Newtonian fluid matrices

In this section the creeping flow of random arrays of spheres surrounded by a Newtonian fluid is studied. Fig. 2 shows our finite-volume simulation results for the dimensionless drag force $\langle F \rangle$ in a random array of spheres, immersed on a Newtonian fluid, at solid volume fractions up to $\phi = 0.2$.

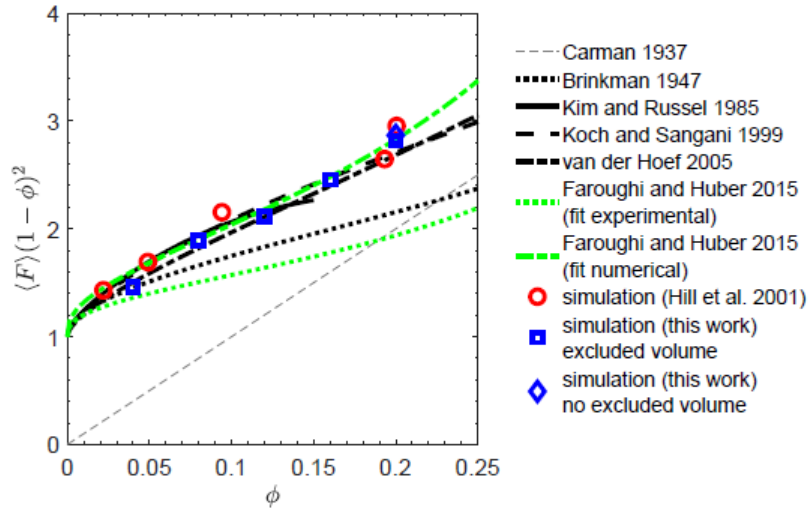


Figure 2. The average value of the dimensionless drag force (multiplied by the porosity squared) for creeping flow of a Newtonian fluid past an array of spheres as a function of the packing fraction ϕ for $n_c = 5$ different configurations. The symbols represent the simulation data, from this work (squares and diamond) and Hill et al. [2] (circles). Also shown are the correlations by Carman [3] (grey line), Brinkman [4] (dotted line), Kim and Russel [5] (solid line), Koch and Sangani [6] (dashed line), van der Hoef et al. [7] (dotted-dashed line) and Faroughi and Huber [8] (green lines).

3.2. Study: drag force within an Oldroyd-B fluid

We performed finite volume simulations of viscoelastic creeping flows (with the Oldroyd-B constitutive equation) past fixed random configurations of particles at Weissenberg numbers up to $Wi = 4$ and for solid volume fractions in the range $0 < \phi \leq 0.2$.

With the purpose of finding a closure model for the drag force exerted by an Oldroyd-B fluid on random arrays of particles at creeping flow conditions and retardation ratio $\beta = 0.5$, in Fig. 3(a) we show the dimensionless average drag force, $\langle F(\phi, Wi) \rangle$. Additionally, in Fig. 3(b) we show the values of the normalized drag force, $\langle F(\phi, Wi) \rangle / F^0(Wi)$. $F^0(Wi)$ represents the drag force exerted by the Oldroyd-B fluid in a single particle, as described in Faroughi et al. [9]. The numerical results presented in Figure 3(b) show that the normalized drag force can be considered independent from the Weissenberg number. This way, we propose fitting an equation to the viscoelastic results as shown in Figure 3(b).

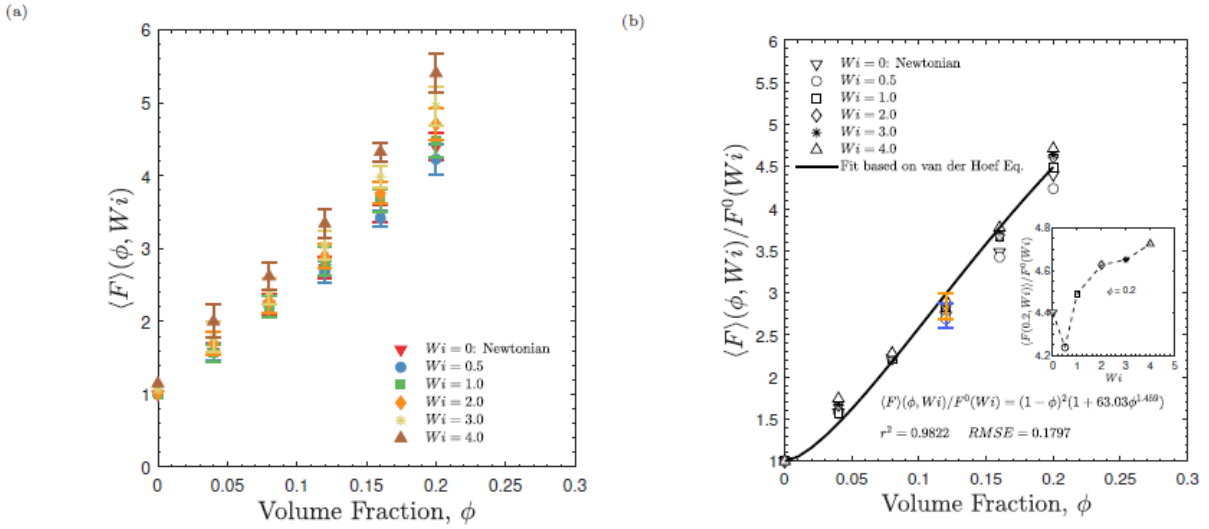


Figure 3. Variation of (a) dimensionless average drag force $\langle F(\phi, Wi) \rangle$ and (b) normalized drag force $\langle F(\phi, Wi) \rangle / F^0(Wi)$ with Weissenberg number for random arrays of fixed particles with solid volume fractions $0 < \phi \leq 0.2$ within an Oldroyd-B viscoelastic matrix-based fluid.

4. Conclusions

Direct numerical simulations (DNS) of random arrays of spherical particles immersed in Newtonian and viscoelastic fluids were performed using a finite-volume method. Additionally, the drag force on individual particles were monitored with the aim to provide an approximate closed form model to describe the numerical simulation data obtained for the unbounded flow of Newtonian and Oldroyd-B fluid past random arrays of spheres, which is required to be integrated in a Eulerian-Lagrangian solver that performs well over a wide range of kinematic conditions.

Acknowledgments: This work is funded by FEDER funds through the COMPETE 2020 Programme and National Funds through FCT (Portuguese Foundation for Science and Technology) under the projects UID-B/05256/2020, UID-P/05256/2020, APROVA-Aprendizagem PROfunda na modelação de escoamentos com fluidos de matriz Viscoelástica Aditivados com partículas (POCI-01-0145-FEDER-016665). The authors would like to acknowledge the Minho University cluster under the project NORTE-07-0162-FEDER-000086 (URL: <http://search6.di.uminho.pt>), the Minho Advanced Computing Center (MACC) (URL: <https://macc.fccn.pt>), the Texas Advanced Computing Center (TACC) at The University of Texas at Austin (URL: <http://www.tacc.utexas.edu>) and the Gcompute HPC Cloud Platform (URL: <https://www.gcompute.com>) for providing HPC resources that have contributed to the research results reported within this paper.

References

- [1] K. D. Housiadas and R. I. Tanner. A model for the shear viscosity of non-colloidal suspensions with Newtonian matrix fluids. *Rheol Acta*, 53:831-841, 2014.

- [2] R. J. Hill, D. L. Koch, and A. J. C. Ladd. The first effects of fluid inertia on flows in ordered and random arrays of spheres. *J. Fluid Mech.*, 448:213-241, 2001.
- [3] P. C. Carman. Fluid flow through granular beds. *Trans. Inst. Chem. Engrs. Lond.*, 15:150-166, 1937.
- [4] H. C. Brinkman. A calculation of the viscous force exerted by a flowing fluid on a dense swarm of particles. *Appl. Sci. Res. A*, 1:27-34, 1947.
- [5] S. Kim and W. B. Russel. Modelling of porous media by renormalization of the Stokes equations. *J. Fluid Mech.*, 154:269-286, 1985.
- [6] D. L. Koch and A. S. Sangani. Particle pressure and marginal stability limits for homogeneous monodisperse gas fluidized bed: kinetic theory and numerical simulations. *J. Fluid Mech.*, 400:229-263, 1999.
- [7] M. A. van der Hoef, R. Beetstra, and J. A. M. Kuipers. Lattice-Boltzmann simulations of low-Reynolds-number flow past mono- and bidisperse arrays of spheres: results for the permeability and drag force. *J. Fluid Mech.*, 528:233-254, 2005.
- [8] S. A. Faroughi and C. Huber. Unifying the relative hindered velocity in suspensions and emulsions of nondeformable particles. *Geophysical Research Letters*, 42:53-59, 2015.
- [9] S. A. Faroughi, C. Fernandes, J. Miguel Nóbrega, and G. H. McKinley. A closure model for the drag coefficient of a sphere translating in a viscoelastic fluid. *Journal of Non-Newtonian Fluid Mechanics*, 277: 104218, 2020.